Corrosion Science 64 (2012) 82–89

Contents lists available at SciVerse ScienceDirect

Corrosion Science

journal homepage: www.elsevier.com/locate/corsci

Inhibitive action of gramine towards corrosion of mild steel in deaerated 1.0 M hydrochloric acid solutions

G. Quartarone *, L. Ronchin, A. Vavasori, C. Tortato, L. Bonaldo

Department of Molecular Sciences and Nanosystems, University Ca' Foscari of Venice, Dorsoduro 2137, 30123 Venice, Italy

ARTICLE INFO

Article history:
Received 22 November 2011
Accepted 12 July 2012
Available online 21 July 2012

Keywords:
A. Mild steel
C. Acid Inhibition
Electrochemical impedance spectroscopy
B. Polarisation

ABSTRACT

The effect of addition of gramine on mild steel dissolution in deaerated 1.0 M hydrochloric acid was studied through potentiodynamic polarisation curves, electrochemical impedance spectroscopy and gravimetric measurements in the temperature range from 25 °C to 55 °C. Gramine was found to shift the corrosion potentials towards less noble values and decrease both dissolution of mild steel and hydrogen evolution reaction. Gramine did not affect the corrosion reaction mechanism (blocking effect). Results obtained from the several measurement techniques were in good agreement and revealed good inhibition efficiencies in the concentration range (0.75 mM ÷ 7.5 mM) particularly at higher concentrations.

1. Introduction

Corrosion is costly and severe materials science problem. The corrosion of mild steel is the most common form of corrosion, especially in acid solution. It has received a considerable attention as a result of its industrial importance, for example in the chemical cleaning and processing, oil well acidizing, petrochemical industry. Mild steel which is subjected to painting, electroplating, phosphate coating, cold rolling, must have a clean surface free from oxide scale. To remove unwanted scale, the mild steel is immersed in an acid solution namely in an acid pickling bath. Hydrochloric acid solutions are by far the most widely used in pickling bath of mild steel. Because of the general aggressiveness of acid solutions, organic inhibitors are commonly used to reduce the corrosion attack on metallic materials [1]. Among the inhibitors which are effective in acid solutions there are nitrogen containing compounds such as derivatives of amines [2–4] pyridazine [5], quinoline and pyridine [6], pyrazole [7,8], pyrazine [9], acridine [10], benzimidazole [11–13] and triazole [14–19]. Previous studies have shown that indole and some its derivatives display good inhibiting effects on steel and copper corrosion in acid solutions [20–28]. It is generally accepted that the primary step in the protecting action of an inhibitor in the acid metal corrosion is adsorption of the organic molecule onto the metal surface, which is usually oxide-free. The adsorption requires the existence of attractive forces between the metal surface (adsorbent) and the organic molecule (adsorbate). According to the type of forces, adsorption can be physisorption, chemisorption or a combination of both [29,30]. Physisorption is weak undirected interaction and is due to electrostatic attraction between inhibiting organic ions or dipoles and the electrically charged surface of metal. The potential of zero charge plays an important role in the electrostatic adsorption process [31]. The charge on metal surface can be expressed in terms of potential difference (φ) between the corrosion potential (E_{corr}) and the potential of zero charge (E_{pzc}) of the metal [$(\varphi) = E_{corr} - E_{pzc}$]. At E_{pzc} the net charge on the metal is zero. At potentials more positive than E_{pzc} the metal is positively charged and at potentials more negative than E_{pzc} the metal is negatively charged. If φ is negative adsorption of cations is favourite. On the contrary the adsorption of anions is favourite if φ is positive. This occurs in the case of inorganic or organic ions as well as dipoles. A peculiarity of physisorption is that the ions or dipoles are non in direct physical contact with the metal. A layer of water molecules separates the metal from the ions or dipoles. Physisorption involves rapid interaction between adsorbent and adsorbate but it is also easily removed from surface with the temperature increase.

Chemisorption involves charge sharing or charge transfer from the adsorbate to adsorbent in order to form a coordinate type of bond. The adsorbent is in contact with the metal surface. It may take place in presence of heteroatoms (P, Se, S, N, O) with lone-pair electrons and/or π electrons due to the presence of multiple bonds or aromatic rings in the adsorbate. The organic inhibitors used generally have reactive functional groups which can be the sites for the chemisorption process. Chemical adsorption has a higher adsorption energy than physical adsorption and, hence, usually is irreversible. It takes place more slowly than physisorption and the temperature dependence shows higher inhibition efficiencies at higher temperatures [32–35].

* Corresponding author. Tel.: +39 041 2348689; fax: +39 041 2348517.
E-mail address: quartagi@unive.it (G. Quartarone).

0010-938X/$ - see front matter © 2012 Elsevier Ltd. All rights reserved.
http://dx.doi.org/10.1016/j.corsci.2012.07.008

Adsorption of an adsorbate on a metal-solution interface is considered as a substitutional adsorption process between the organic molecule in the aqueous solution, Org(sol) and the water molecules adsorbed on the metallic surface, H2O(ads):

$$Org_{(sol)} + \chi H_2O_{(ads)} = Org_{(ads)} + \chi H_2O_{(sol)} \quad (1)$$

where χ is the size ratio representing the number of water molecules replaced by one molecule of organic adsorbate. The adsorption process (1) reaches equilibrium when the chemical potential on the left side of the equation is equal to that of right. Depending on the means of expressing the chemical potential (site fractions, mole fractions, etc.) various isotherms of adsorption can be derived to describe the adsorption process [36,37].

The most frequently used isotherms to describe the adsorption process are: Langmuir, Frumkin, Hill de Boer, Parsons, Temkin, Flory–Huggins, Dhar-Flory–Huggins, and Bockris-Swinkels [38].

Recently numerous efforts have been realised by research in environmental protection using green chemistry principles. This has been employed specifically in the field of corrosion, resulting in the decreased use of toxic inhibitors and the development of new environmentally friendly ones. Gramine, which occurs in different plant species such as in the sprouting barley and acer saccharinum, is a natural product at low environmental impact and is typical of the simpler indole alkaloids [39]. The aim of the present study was to study the inhibiting action of the gramine on the corrosion of mild steel in deaerated 1.0 M hydrochloric acid solutions in the temperature range of 25–55 °C. The adsorption behaviour of the gramine was also analysed in order to choose the appropriate adsorption isotherm and determine the energy of adsorption.

2. Experimental

In order to study the inhibitive action of the gramine towards the corrosion of mild steel in acid solution, corrosion tests were performed in 1.0 M HCl solutions without or with different concentrations of inhibitor. The composition (w%) of the mild steel used in experimental was: C: 0.092; Mn: 0.239; Al: 0.037; Cr: 0.025; Si: 0.024; S: 0.020; Cu: 0.019; Nb: 0.006; Sn: 0.005; As: 0.0038; V: 0.002; Co: 0.002; Ti: 0.002; B: 0.0014 and balance Fe. The 1.0 M hydrochloric acid solutions were prepared from reagent grade concentrated acid and distilled water. Gramine (99%) was used in this study as purchased from the Aldrich. The compound was dissolved in 1.0 M HCl at various concentrations (from 0.75 mM ÷ to 7.5 mM). The chemical structure of gramine is shown in Fig. 1.

A mild steel cylinder pressed into a Teflon holder acted as a working electrode. Its working area of 1 cm^2 remained precisely fixed. Prior to each experiment the surface of working electrode was abraded sequentially with 120–320–600–800–1200 grade emery paper, rinsed with distilled water, degreased with acetone, dried with a stream of air. The electrode was then immediately inserted into a glass cell ASTM [40] containing 700 ml of the aggressive solution, deaerated by prolonged bubbling with pure nitrogen (12 h), without or the desired concentration of the investigated inhibitor. A saturated calomel electrode (SCE), provided with a Luggin capillary probe, was used as reference electrode while platinum electrodes were used as counters. The tip of the Luggin capillary is made very close to the surface of the working electrode to minimize IR drop. Before each electrochemical impedance and Tafel experiments, the electrode was allowed to corrode freely and its open circuit potential (OCP) was recorded as a function of time from 2 h to 5 h according to the temperature and inhibitor concentration. After reaching a stable value for the open circuit potential (E_{corr}), electrochemical impedance measurements were performed at temperature of 25 °C; 35 °C; 45 °C and 55 °C. Electrochemical impedance measurements are performed, in the absence (blank test solution) and presence of various concentrations of gramine, with an a.c. voltage amplitude of 5 mV using an EGG PAR Potentiostat Model 263 with a Lock-in Amplifier Model 5210 PC-controlled with an EGG software package. The frequency range is swept between 100 kHz and 10 mHz with 10 point per hertz decade.

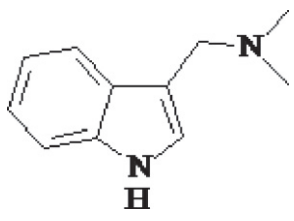

3-(dimethylaminomethyl)-indole

Fig. 1. Chemical structure and IUPAC name of the gramine.

Polarisation curves were recorded after the electrochemical impedance measurements on the same electrode without any surface treatment at 25 °C; 35 °C; 45 °C and 55 °C using the same EGG Potentiostat. The potential was scanned from −180 mV to + 180 mV versus E_{corr} with the scan rate of 200 μV/S.

Weight-loss measurements were carried out using a thermostated 1.0 litre double-walled glass cell. The mild steel specimens were 30 mm × 40 mm × 3 mm in size. The specimens before each test, were placed in 1.0 M hydrochloric acid solutions for 1 h to homogenise the surface, then were washed, dried, weighed and plunged into the deaerated solution (1000 mL) thermostated at 25 °C; 35 °C; 45 °C and 55 ± 0.1 °C respectively. After two hours the specimens were removed, washed with distilled water, dried and reweighed to determine the overall weight loss. All measurements were repeated three times to check reproducibility.

3. Results

3.1. Weight loss measurements

Table 1 gives the inhibition efficiencies (I.E. = $\theta \times 100$) and the gravimetric corrosion rates (R_{corr}) of mild steel in deaerated 1.0 M hydrochloric acid solutions at 25 °C; 35 °C; 45 °C and 55 °C.

The corrosion rates were expressed mg/cm^2 × h and were calculated using the following equation:

$$R_{corr} = \frac{m1 - m2}{A \times t} \quad (2)$$

where $m1$ is the initial weight before immersion, $m2$ the final weight after the corrosion test, A the geometrical surface area (28.2 cm^2), and t the period of corrosion test (2 h). The surface coverage degree (θ) for different concentrations of inhibitor has been evaluated from corrosion rate measurements using the following equation:

$$\theta = \frac{R_0 - R_{inh}}{R_0} \quad (3)$$

where R_0 and R_{inh} are the values of the corrosion rates of mild steel after immersion in uninhibited and inhibited, respectively. It can be seen that the addition of gramine strongly suppressed the corrosion of mild steel in 1.0 M hydrochloric acid solutions at the higher concentrations. The inhibition efficiencies increased with inhibitor concentration in the temperature range of 25–55 °C, reaching a maximum value of 98% at 7.5 mM and 55 °C. By increasing the inhibitor concentration, the part of metal surface covered by inhibitor molecules increases and that leads to an increase in the inhibition efficiencies.

Table 1
Inhibition efficiencies (I.E.) and gravimetric corrosion rates (R_{corr}) of mild steel in deaerated 1.0 M HCl at 25 °C; 35 °C; 45 °C and 55 °C.

C (mM)	R_{corr} (mg/cm^2 × h)	I.E.	R_{corr} (mg/cm^2 × h)	I.E.	R_{corr} (mg/cm^2 × h)	I.E.	R_{corr} (mg/cm^2 × h)	I.E.
	25 °C		35 °C		45 °C		55 °C	
0	20.2×10^{-2}	–	39.1×10^{-2}	–	5.3×10^{-1}	–	13.4×10^{-1}	–
0.75	12.5×10^{-2}	38	25.4×10^{-2}	35	3.7×10^{-1}	31	8.4×10^{-1}	37
1.0	9.3×10^{-2}	54	20.3×10^{-2}	48	2.6×10^{-1}	51	6.4×10^{-1}	52
2.0	6.2×10^{-2}	70	9.8×10^{-2}	75	1.6×10^{-1}	70	3.8×10^{-1}	72
3.0	2.6×10^{-2}	87	5.9×10^{-2}	85	8.5×10^{-2}	84	2.1×10^{-1}	84
4.0	1.8×10^{-2}	91	3.9×10^{-2}	90	4.7×10^{-2}	91	1.1×10^{-1}	92
5.0	1.4×10^{-2}	93	2.7×10^{-2}	93	2.6×10^{-2}	95	8.0×10^{-2}	94
7.5	1.0×10^{-2}	95	1.6×10^{-2}	96	1.6×10^{-2}	97	2.7×10^{-2}	98

3.2. Polarisation curves

Figs. 2 and 3 show some typical anodic and cathodic potentiodynamic polarisation curves at 35 °C and 55 °C in deaerated 1.0 M HCl solutions without and with different concentrations of gramine.

The corrosion kinetic parameters obtained from these curves such as corrosion potentials (E_{corr}); corrosion current densities (i_{corr}) determined by extrapolation of the cathodic and anodic Tafel lines to the corrosion potential; cathodic and anodic Tafel slopes (b_c and b_a); corrosion rates (R_{corr}); surface coverage degrees (θ) calculated by the following equation:

$$\theta = 1 - \frac{(i_{corr})1}{(i_{corr})2.} \quad (4)$$

where $(i_{corr})1$ and $(i_{corr})2$ are the corrosion current densities with and without inhibitor; the inhibition efficiencies are given in Table 2.

The results reported reveal the strong inhibiting effect of the gramine at the higher concentrations of inhibitor. The more the inhibitor molecules adsorbed on mild steel surface, the bigger the values of surface coverage degree and of inhibitor efficiency. Moreover it can be seen the free corrosion potential shifts towards less noble values when the inhibitor is added. This indicates that gramine affects mainly the cathodic reaction, raising the cathodic overpotential more than the anodic one, i.e. gramine can be defined as a mixed-type inhibitor [41–43]. The anodic and cathodic curves were affected by the inhibitor. In particular, the polarisation curves when the inhibitor was added were shifted towards lower current densities with respect to the uninhibited one, generally retaining the same trend. As can be seen in Table 2, this means that

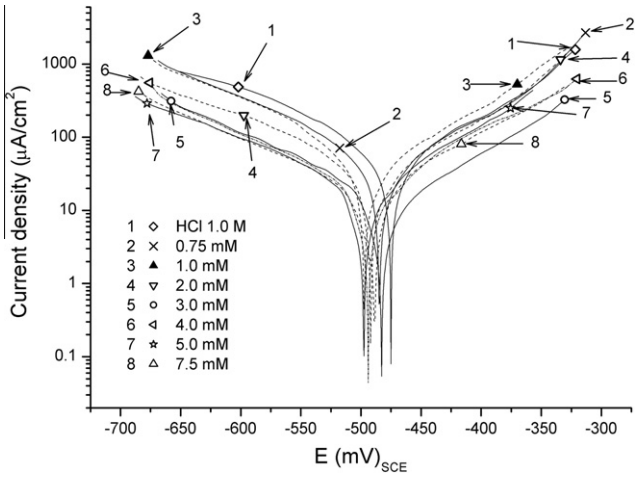

Fig. 2. Anodic and cathodic potentiodynamic polarisation curves for mild steel in deaerated 1.0 M HCl without and with different concentration of gramine at 35 °C.

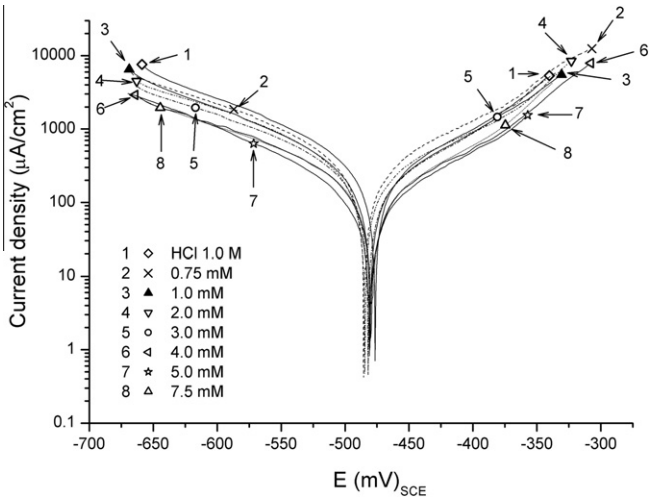

Fig. 3. Anodic and cathodic potentiodynamic polarisation curves for mild steel in deaerated 1.0 M HCl without and with different concentration of gramine at 55 °C.

the addition of gramine reduced iron anodic dissolution and also retarded the hydrogen evolution reaction. Furthermore, the slope values of Tafel's line, b_c and b_a, remained almost unchanged upon addition of inhibitor. The approximately constant values of the Tafel slopes indicate that gramine does not change the corrosion mechanism of the mild steel in 1.0 M hydrochloric acid solutions i.e. adsorbed inhibitor acts, by simple blocking of active metal sites for both anodic and cathodic processes. In other words, gramine like other adsorption inhibitors, should undergo adsorption in electrical double layer. This limits the accessibility of the surface to the reacting ion H_3O^+, i.e. the gramine blocks part of the metal surface with respect to the corrosive medium and hence decreases the reaction rate without affecting the reaction mechanism [44,45].

3.3. Electrochemical impedance spectroscopy (EIS)

The effect of different concentration of gramine on corrosion of mild steel in 1.0 M hydrochloric acid solutions at 25; 35; 45 and 55 °C by electrochemical impedance measurements was also studied. Some Nyquist plots are shown in Figs. 4 and 5.

It can be that the impedance response contains a single capacitive loop, corresponding to one time constant, whose size increased by increasing the concentration of gramine. The capacitive loop was attributed to a faradic process involving a charge transfer resistance in parallel with double-layer capacitance element [46]. This indicated that inhibitor molecules more and more adsorbed on the mild steel surface by increasing their concentration. Consequently gramine increased the charge transfer

Table 2
Electrochemical data obtained from Tafel plots for mild steel in deaerated 1.0 M HCl with different gramine concentrations at 25 °C; 35 °C; 45 °C and 55 °C.

T °C	C (mM)	E_{corr} (mV_{SEC})	i_{corr} ($\mu A/cm^2$)	b_c (mV/dec)	b_a (mV/dec)	R_{corr} ($mg/cm^2 \times h$)	θ	I.E.
25	0	−470	154	−98	62	6.8×10^{-2}		
	0.75	−472	94	−105	61	4.1×10^{-2}	0.39	39
	1.0	−477	55	−115	55	2.4×10^{-2}	0.64	64
	2.0	−477	31	−107	76	1.3×10^{-2}	0.80	80
	3.0	−502	22	−115	72	9.5×10^{-3}	0.86	86
	4.0	−513	15	−111	80	6.5×10^{-3}	0.90	90
	5.0	−14	11	−106	100	4.7×10^{-3}	0.93	93
	7.5	−518	8	−114	101	3.5×10^{-3}	0.95	95
35	0	−470	328	−107	66	1.4×10^{-1}		
	0.75	−469	197	−123	66	8.6×10^{-2}	0.40	40
	1.0	−468	118	−114	56	5.1×10^{-2}	0.64	64
	2.0	−473	66	−111	82	2.9×10^{-2}	0.80	80
	3.0	−492	39	−115	86	1.7×10^{-2}	0.88	88
	4.0	−489	33	−116	84	1.4×10^{-2}	0.90	90
	5.0	−498	20	−118	82	8.6×10^{-3}	0.94	94
	7.5	−500	13	−121	81	5.6×10^{-3}	0.96	96
45	0	−475	560	−141	70	5.7×10^{-1}		
	0.75	−476	308	−156	78	3.1×10^{-1}	0.45	45
	1.0	−478	196	−137	77	2.0×10^{-1}	0.65	65
	2.0	−480	140	−149	75	1.4×10^{-1}	0.75	75
	3.0	−482	56	−130	84	5.7×10^{-2}	0.90	90
	4.0	−487	37	−147	85	3.4×10^{-2}	0.94	94
	5.0	−479	22	−145	80	2.3×10^{-2}	0.96	96
	7.5	−494	17	−141	68	1.6×10^{-2}	0.97	97
55	0	−475	1382	−115	78	14.4×10^{-1}		
	0.75	−477	857	−128	88	8.9×10^{-1}	0.38	38
	1.0	−476	719	−120	75	7.5×10^{-1}	0.48	48
	2.0	−480	498	−118	62	5.1×10^{-1}	0.64	64
	3.0	−479	276	−111	66	2.8×10^{-1}	0.80	80
	4.0	−478	138	−125	81	1.4×10^{-1}	0.90	90
	5.0	−483	111	−130	87	1.1×10^{-1}	0.92	92
	7.5	−485	55	−128	89	5.5×10^{-2}	0.96	96

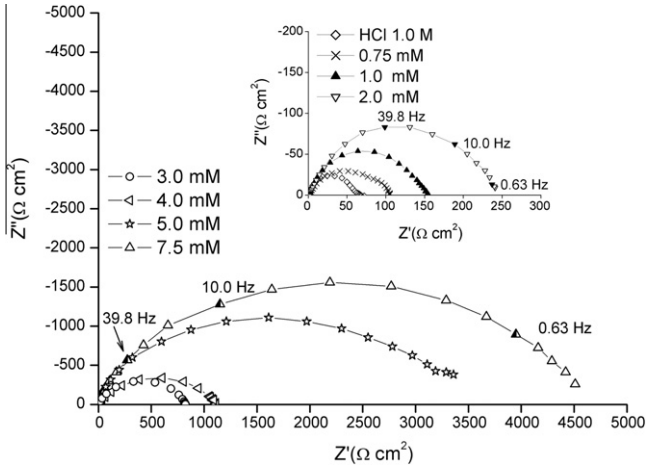

Fig. 4. Nyquist plots for mild steel corrosion in 1.0 M HCl at 25 °C containing different concentrations of gramine.

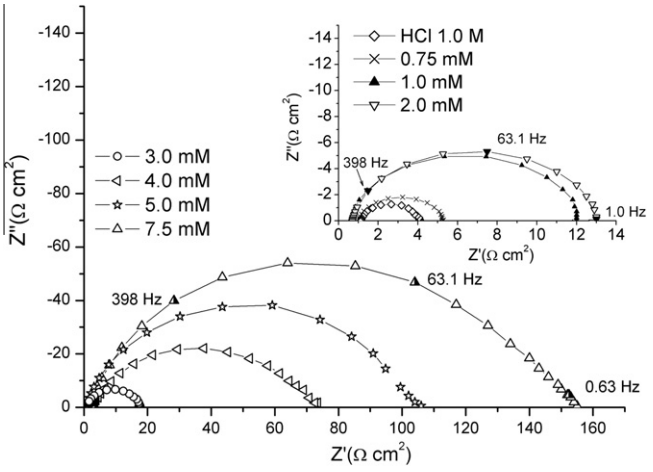

Fig. 5. Nyquist plots for mild steel corrosion in 1.0 M HCl at 55 °C containing different concentrations of gramine.

resistance at the electrode–electrolyte interface and then it had an increasing inhibition action on mild steel corrosion in 1.0 M hydrochloric acid solutions. It can be also noticed that the impedance spectra showed a depressed form of the capacitive loop. The centre of the experimental arc was displaced below the real axis. This phenomenon was related to the surface heterogeneity due to the microscopic roughness of the electrode surface and inhibitor adsorption [47–49]. The equivalent circuit of Fig. 6 fits well our experimental results.

In that equivalent circuit, R_s is the solution resistance, R_{ct} is the charge transfer resistance, and CPE is the constant phase element whose impedance is defined by the mathematical expression [50]:

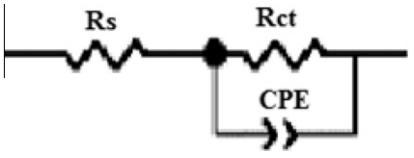

Fig. 6. Electrochemical equivalent circuit used in fitting impedance data for mild steel corrosion in 1.0 M HCl in absence and presence of different concentration of gramine.

Table 3
Electrochemical data obtained from Nyquist plots for mild steel corrosion in deaerated 1.0 M HCl with different gramine concentrations at 25 °C; 35 °C; 45 °C and 55 °C.

T (°C)	C (mM)	C_{dl} (F/cm^2)	n	R_s ($\omega \times$ cm^2)	R_{ct} ($\omega \times$ cm^2)	θ	I.E.
25	0	7.55×10^{-5}	0.87	0.83	66		
	0.75	5.74×10^{-5}	0.86	1.24	105	0.37	37
	1.0	7.59×10^{-6}	0.79	1.25	158	0.58	58
	2.0	1.76×10^{-5}	0.78	1.31	242	0.73	73
	3.0	1.90×10^{-6}	0.73	0.73	823	0.92	92
	4.0	2.27×10^{-5}	0.73	0.72	1114	0.94	94
	5.0	1.06×10^{-5}	0.82	1.39	3151	0.98	98
	7.5	9.50×10^{-6}	0.76	1.41	4580	0.99	99
35	0	1.45×10^{-4}	0.91	1.47	28.0		
	0.75	4.24×10^{-5}	0.79	1.02	41.9	0.33	33
	1.0	7.43×10^{-5}	0.91	1.49	52.9	0.47	47
	2.0	5.91×10^{-5}	0.89	0.81	96	0.71	71
	3.0	3.11×10^{-5}	0.82	1.29	191	0.85	85
	4.0	6.34×10^{-6}	0.70	1.06	306	0.91	91
	5.0	5.01×10^{-6}	0.72	0.96	413	0.93	93
	7.5	4.94×10^{-6}	0.70	1.30	666	0.96	96
45	0	2.23×10^{-4}	0.91	1.23	12.0		
	0.75	6.50×10^{-5}	0.86	0.87	15.6	0.23	23
	1.0	1.07×10^{-4}	0.90	0.72	21.9	0.45	45
	2.0	6.38×10^{-5}	0.77	0.57	58	0.79	79
	3.0	5.57×10^{-5}	0.83	1.03	71	0.83	83
	4.0	1.15×10^{-5}	0.78	2.73	168	0.93	93
	5.0	3.12×10^{-5}	0.85	1.26	253	0.95	95
	7.5	1.06×10^{-5}	0.74	1.27	455	0.97	97
55	0	2.82×10^{-4}	0.90	1.11	3.0		
	0.75	3.42×10^{-4}	0.91	1.06	4.8	0.38	38
	1.0	1.60×10^{-4}	0.93	0.60	6.8	0.56	56
	2.0	1.58×10^{-4}	0.91	0.69	10.7	0.72	72
	3.0	6.20×10^{-5}	0.86	0.85	18.9	0.84	84
	4.0	1.44×10^{-5}	0.71	2.62	59	0.95	95
	5.0	7.12×10^{-5}	0.82	0.84	97	0.97	97
	7.5	7.15×10^{-6}	0.78	1.25	153	0.98	98

$$Z_{CPE} = \frac{1}{T \times (j\omega)^{n.}} \quad (5)$$

where T is the double-layer capacitance quantity; j is $(-1)^{1/2}$; ω is angular frequency; n an exponent related to the phase angle. The exponent n is <1 and for the electrode–electrolyte interfaces usually assumes the values: $1 > n > 0.8$ [51]. Considering that the impedance of a double-layer does not behave as an ideal capacitor, constant phase element is most often used to describe the frequency dependence of non ideal capacitive behaviour [52]. The non ideal double-layer capacitance depends on the electrode material, its surface preparation and whether or not absorbable molecules are present in the electrolyte solution. The deviations from ideal capacitance behaviour of the double layer at electrodes often become apparent at such electrodes where a faradic resistance is coupled with the capacitance. Consequently, instead of regular semicircular complex-plane plots, the Nyquist plots are arcs of semicircles, i.e. with centres depressed below Z' axis. The smoother and cleaner the electrode surface, the closer is the value of n to unity i.e. the closer to ideal capacitive behaviour [53]. The values of some elements fitted using the circuit of Fig. 6 are listed in Table 3.

The data of n were generally lower in the inhibited solutions than that uninhibited ones. This is an indication that the inhibitor contributes to increase surface heterogeneity due to its adsorption at electrode–electrolyte interface [54]. The values of capacitance (C_{dl}) were calculated by the relation [50]:

$$C_{dl} = \sqrt[n]{T \times R_{ct}^{(1-n)}} \quad (6)$$

where R_{ct} charge transfer resistance, is a measure of the electron transfer across the electrode–electrolyte interface and it is inversely proportional to corrosion rate [55]. Table 3 shows that by increasing the gramine concentration the charge transfer resistance increased. The adsorption of gramine molecules on electrode–electrolyte interface modifies the interface structure and that can bring about an increase of R_{ct}. Really the resulting inhibitor adsorption can insulate in some way the mild steel surface from the corrosive medium.

Inhibition efficiency for different inhibitor concentrations was calculated according to following relation [56]:

$$I.E. = [(R_{ct} - R_{ct}^0) \div R_{ct}] \times 100 \quad (7)$$

where R_{ct} and R_{ct}^0 are the charge transfer resistances in the inhibited and uninhibited solutions respectively. Fig. 7 shows the effect of

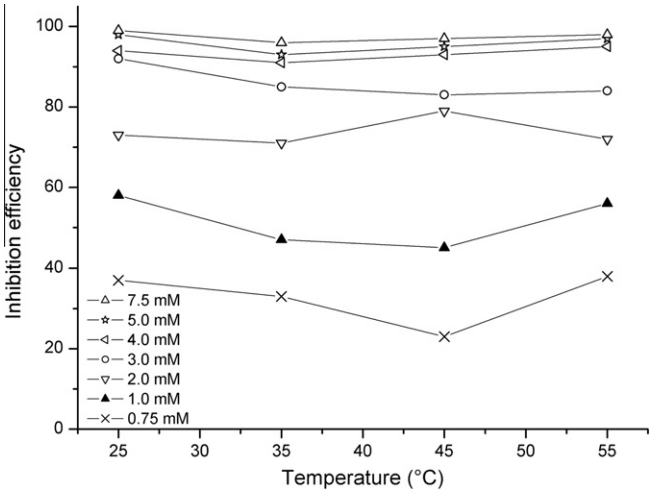

Fig. 7. Effect of temperature on the inhibition efficiency of gramine in the mild steel corrosion in 1.0 M HCl at 25 °C; 35 °C; 45 °C and 55 °C.

temperature on the inhibition efficiency of gramine in the mild steel corrosion in 1.0 M HCl solutions at 25; 35; 45 and 55 °C.

In the temperature range of 25–55 °C can be seen that inhibition efficiency increased as the inhibitor concentration increased. Moreover at same inhibitor concentration the inhibition efficiency is almost unchanging in the temperature range of 25–55 °C. That could indicate a relatively strong inhibitor-metal bond, like chemisorption.

4. Discussion

4.1. Effect of temperature

The effect of temperature can be accomplished by investigating the temperature dependence of the corrosion rates (see Table 2) obtained using Tafel extrapolation method. In the studied temperature range, the corrosion rates were found to increase with the increase in the temperature for both inhibited and uninhibited acid solutions while they decreased with the increase of inhibitor concentration for a given temperature. The temperature dependence of the corrosion rate (R_{corr}) can be expressed by Arrhenius equation:

$$R_{corr} = k.exp(-\frac{E}{RT}) \quad (8)$$

where k is the corrosion rate constant, E is the activation energy, T is the absolute temperature and R is the universal gas constant. This equation can be represented graphically by plotting natural logarithm of the corrosion rates vs. $1/T$ without and with addition of various concentrations of gramine. The plots obtained were rough straight lines with linear regression coefficients from 0.94 to 0.98. The E values were calculated from the slope, equals to $-E/R$ of each straight line. Arrhenius plots are shown in Fig. 8 and values of E are listed in Table 4.

It can be seen that at lower concentrations the activation energy increased. This could be interpreted as physical adsorption which occurs in the first stage [57,58]. At highest concentration, activation energy was found to decrease and these data agree with those reported in literature [59]. Unchanged or lowered activation energy is related to the existence of chemisorption [60]. The results obtained in the study could be interpreted by considering that at lower concentrations physisorption of gramine could be the prevailing mechanism and chemisorption at higher concentrations [61].

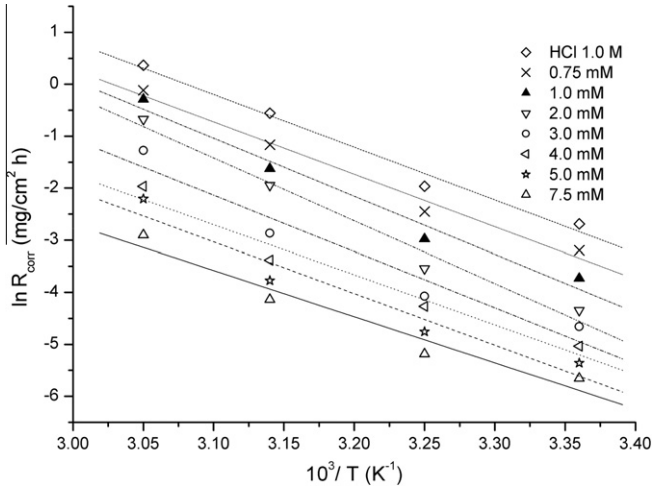

Fig. 8. The relationship between ln R_{corr} and 1/T for mild steel in 1.0 M HCl in presence of various concentrations of gramine.

Table 4
Activation energies at various concentrations of gramine for mild steel corrosion in deaerated 1.0 M HCl.

Inhibitor concentration (mM)	Activation energy (kJ/mol)
0	84.3
0.75	83.8
1.0	92.8
2.0	100.4
3.0	89.9
4.0	80.0
5.0	82.6
7.5	73.8

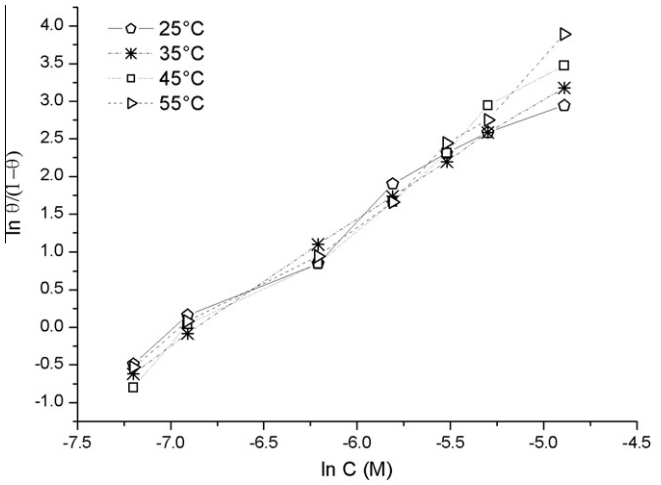

Fig. 9. Langmuir's adsorption plots for gramine on the mild steel surface in 1.0 M HCl at 25 °C; 35 °C; 45 °C and 55 °C.

Table 5
Data from Langmuir's isotherms for gramine on the mild steel surface in 1.0 M HCl at 298 °K; 308 °K; 318 °K and °K.

Temperature (°K)	ln k(1/M)	$-\Delta G^0_{ads}$(kJ/mol)
298	10.64	36.32
308	11.31	39.26
318	12.44	43.52
328	12.54	45.16

4.2. Adsorption isotherm

Information on the interaction between the inhibitor molecules and the metal surface can be provided by adsorption isotherm. The inhibition efficiencies by electrochemical impedance spectroscopy had the same trend of those obtained by both the potentiodynamic polarisation curves and the weight loss measurements (see Tables 1–3). The data of weight loss, obtained by means of directed method, are more reliable than the indirect methods, like Tafel polarisation curves and electrochemical impedance spectroscopy. Therefore the surface coverage degrees calculated from weight loss measurements and corresponding to different concentrations of gramine in the 25–55 °C temperature range, were used to study the adsorption behaviour of gramine and to choose the more suitable adsorption isotherm. Attempts were made to fit these values to various isotherms above-mentioned. The correlation coefficient was used to choose the isotherm that best fits the experimental data. The Langmuir's adsorption isotherm was found to be the best description of the adsorption behaviour of gramine on mild steel.

The Langmuir's isotherm can be written as follows:

$$\ln\frac{\theta}{1-\theta} = \ln K + \ln C \quad (9)$$

where θ is the degree of surface coverage, C the molar inhibitor concentration in the bulk solution and k is the equilibrium constant of the process of adsorption which is correlated to the standard free energy $(-\Delta G^0_{(ads)})$ by the relation:

$$K = \frac{1}{55.5} exp(\frac{-\Delta G^0_{(ads)}}{RT}) \quad (10)$$

where 55.5 is the molar concentration of water in the solution [38].

The linear relationships of $\ln \frac{\theta}{1-\theta}$ versus $\ln C$ at temperatures of 25 °C; 35 °C; 45 °C and 55 °C according to Langmuir's isotherm is displayed in Fig. 9.

The values of $\ln k$ obtained from the Langmuir's adsorption isotherm are listed in Table 5, together with the values of the standard free energy of adsorption, $(-\Delta G^0_{(ads)})$.

The negative values of $(-\Delta G^0_{(ads)})$ suggest that the gramine was spontaneously adsorbed on electrode–electrolyte interface.

It has been reported that values of $(-\Delta G^0_{(ads)})$ up to −20 kJ/mol are consistent with the physisorption; those around −40 kJ/mol or higher are consistent with chemisorption [38] and [62]. The high values of $(-\Delta G^0_{(ads)})$ and relative increase with temperature in the range of 25–55 °C suggest a chemisorption. Gramine is a nitrogen-containing organic compound having both unshared electron pair and π-electrons. In 1.0 M hydrochloric acid solutions gramine is protonated through amino nitrogen, leading to positive charge in the molecule.

It has been determined the value of −530 mV_{SEC} for E_{pzc} of the mild steel in 1.0 M hydrochloric acid solutions [31]. Considering the E_{corr} values reported in Table 2, the mild steel surface is positively charged and consequently it is difficult for the protonated gramine to approach the metal surface. In the presence of chloride ions, having a smaller degree of hydration, the specific adsorption is expected to be pronounced. Being specifically adsorbed, they create an excess negative charge towards the solution and favour the electrostatic adsorption of the cations [63]. Thus, by means of electrostatic attraction, portonated gramine can reach mild steel-solution interface, be easily adsorbed and could transfer π electrons from the aromatic gramine ring to the d-orbital of iron atom. So, in the process of adsorption both physisorption and chemisorption might take place [30].

4.3. Effect of inhibitor on the capacitance

The data of Table 3 show that in general the magnitude of C_{dl}, calculated by relation (6), decreases with increasing inhibitor concentration. The decrease in C_{dl} could be in relation to the adsorption of inhibitor molecules at solution-metal interface [29]. According to the parallel-plate model for the electrical double-layer:

$$C_{dl} = \frac{\varepsilon}{4\pi d} \quad (11)$$

where C_{dl} is the capacitance per unit area of the condenser plates, d is the distance between the plates i.e. thickness of the electric double-layer, and ε is the dielectric constant of material between the plates [64]. The decrease of C_{dl} could be due to an increase in the thickness of the electrical double-layer and/or to a local dielectric constant decrease. Increase of d could be caused from the substitution of water molecules by adsorbed gramine. The dielectric constant of water is dependent on the electric field strength of the environment at solution-metal interface. The electric field due the adsorbed ions and/or organic dipoles orients the water molecules and their degree of orientation affects his electric constant. The more water is oriented, i.e. the more water dipoles are aligned, the lower is the dielectric constant. Adsorbed organic molecules having $-COO^-$, $-OH^-$, $-NH_3^+$ groups and / or π electron system can lower the water mobility and consequently the dielectric constant [65]. Therefore it can be assumed that the dielectric constant decrease can be caused by orientation forces of the π-electron system and/or protonated inhibitor. In conclusion, the observed electrical properties of the gramine molecule in the double layer is consistent with physisorption and chemisorption of the inhibitor.

5. Conclusion

1. Gramine displayed good inhibitive properties towards the corrosion of mild steel in 1.0 M hydrochloric solutions in the temperature range of 25–55 °C.
2. Data obtained from weight loss and electrochemical measurements have shown that the inhibiting effect of inhibitor increased by increasing its concentration.
3. Results of potentiodynamic polarisation curves indicated that gramine is a mixed-type inhibitor which affected both the anodic and cathodic reactions by simple blocking of the active metal sites, i.e. gramine did not change the corrosion mechanism of the mild steel in 1.0 M hydrochloric acid solutions.
4. The adsorption behaviour of gramine followed the Langmuir's isotherm.
5. Both physisorption and chemisorption seemed to contribute to the adsorptive behaviour of the inhibitor.

References

[1]] W. Machu, in: Proceedings 3rd Europ. Symp. on corrosion inhibitors, Univ. of Ferrara, Ferrara, Italy, 1970, pp. 107–117.
[2] G. Schmitt, Application of inhibitors for acid media, Br. Corros. J. 19 (1984) 165–175.
[3] S.L. Granese, Study of the inhibitory action nitrogen-containing compounds, Corrosion 44 (1988) 322–327.
[4] H. Luo, Y.C. Guan, K.N. Han, Corrosion inhibition of a mild steel by aniline and alkylamine in acidic solutions, Corrosion 54 (1998) 721–731.
[5] A. Chetouani, A. Aouniti, B. Hammouti, N. Benchat, T. Benhadda, S. Kertit, Corrosion inhibitors for iron in hydrochloride acid solution by newly synthesised pyridazine derivatives, Corros. Sci. 45 (2003) 1675–1684.
[6] F. Zucchi, G. Trabanelli, G. Brunoro, The influence of the chromium content on the inhibitive efficiency of some organic compounds, Corros. Sci. 33 (1992) 1135–1139.
[7] S.A. Abd EL-Maksoud, Electrochemical studies on the effect of pyrazole-containing compounds on the corrosion of carbon steel in 1 M sulphuric acid, Mater. Corros. 54 (2003) 106–112.
[8] K. Tebbji, H. Oudda, B. Hammouti, M. Benkaddour, M. El Kodadi, F. Malek, A. Ramdani, Inhibitive action of two bipyrazolic isomers towards corrosion of steel in 1 M HCl, Appl. Surf. Sci. 241 (2005) 326–334.
[9] M. Bouklah, A. Attayibat, S. Kertit, A. Ramdani, B. Hammouti, A pyrazine derivative as corrosion inhibitor for steel in sulphuric acid solution, Appl. Surf. Sci. 242 (2005) 399–406.
[10] S.L. Granese, B.M. Rosales, C. Oviedo, J.O. Zerbino, The inhibition action of heterocyclic nitrogen organic compounds on Fe and steel in HCl media, Corros. Sci. 33 (1992) 1439–1453.
[11] A. Popova, E. Sokolova, S. Raicheva, M. Christov, AC and DC study of the temperature effect on mild steel corrosion in acid media in the presence of benzimidazole derivatives, Corros. Sci. 45 (2003) 33–58.
[12] A. Popova, M. Christov, T. Deligeorgiev, Influence of the molecular structure on the inhibitor properties of benzimidazole derivatives on mild steel corrosion in 1 M hydrochloric acid, Corrosion 59 (2003) 756–764.
[13] J. Cruz, T. Pandiyan, E. Garcìa-Ochoa, A new inhibitor for mild carbon steel: Electrochemical and DFT studies, J. Electroanal. Chem. 583 (2005) 8–16.
[14] F. Bentiss, M. Lagrenee, M. Traisnel, B. Mernari, H. El Attari, 3,5-bis(*n*-Hydroxyphenyl)-4-amino-1,2,4-triazoles and 3,5-bis(*n*-aminophenyl)-4-amino-1,2,4-triazole: a new class of corrosion inhibitors for mild steel in 1 M HCl medium, J. Appl. Electrochem. 29 (1998) 1073–1078.
[15] B. Mernari, H. El Attari, M. Traisnel, F. Bentiss, M. Lagrenee, Inhibiting effects of 3,5-bis(*n*-pyridyl)-4-amino-1,2,4-triazoles on the corrosion for mild steel in 1 M HCl medium, Corros. Sci. 40 (1998) 391–399.
[16] M.A. Quraishi, R. Sadar, Aromatic triazoles as corrosion inhibitors for mild stell in acidic environments, Corrosion 58 (2002) 747–756.
[17] F. Bentiss, M. Lagrenee, B. Elmehdi, B. Mernari, M. Traisnel, H. Vezin, Electrochemical and quantum chemical studies of 3,5-di(*n*-tolyl)-4-amino-1,2,4-triazole adsorption on mild steel in acidic media, Corrosion 58 (2002) 399–407.

[18] J. Cruz, E. Garcia-Ochoa, M. Castro, Experimental and theoretical study of the 3-amino-1,2,4-triazole and 2-aminotriazole corrosion inhibitors in carbon steel, J. Electrochem. Soc. 150 (2003) B26–B35.
[19] H.H. Hassan, E. Abdelghani, M.A. Amin, Inhibition of mild steel corrosion in hydrochloric acid solution by triazole derivatives. Part I. Polarisation and EIS studies, Electrochim. Acta 52 (2007) 6359–6366.
[20] G. Moretti, G. Quartarone, A. Tassan, A. Zingales, Inhibiton of mild steel corrosion in 1 N sulphuric acid through indole, Werkst. und Korr. 45 (1994) 641–647.
[21] G. Moretti, G. Quartarone, A. Tassan, A. Zingales, Some derivatives of indole as mild steel corrosion inhibitors in 0. 5 M sulphuric acid, Brit. Corros. J. 31 (1996) 49–54.
[22] G. Moretti, F. Guidi, Tryptophan as copper corrosion inhibitor in 0.5 M aerated sulfuric acid, Corros. Sci. 44 (2002) 1995–2011.
[23] G. Quartarone, T. Bellomi, A. Zingales, Inhibition of copper corrosion by isatin in aerated 0.5 M H_2SO_4, Corros. Sci. 45 (2003) 715–733.
[24] G. Moretti, F. Guidi, G. Grion, Tryptamine as a green iron corrosion inhibitor in 0.5 M deaerated sulphuric acid, Corros. Sci. 46 (2004) 387–403.
[25] G. Quartarone, L. Bonaldo, C. Tortato, Inhibitive action of indole-5-carboxylic acid towards corrosion of mild steel in deaerated 0.5 M sulfuric acid solutions, Appl. Surf. Sci. 252 (2006) 8251–8257.
[26] F. Bentiss, F. Gassama, D. Barbry, L. Gengembre, H. Vezin, M. Lagrenee, M. Traisnel, Enhanced corrosion resistance of mild steel in molar hydrochloric acid solution by 1,4-bis(2-pyridyl)-5H-pyridazino [4,5-b] indole: electrochemical, theoretical and XPS studies, Appl. Surf. Sci. 252 (2006) 2684–2691.
[27] G. Quartarone, L. Bonaldo, M. Battilana, T. Tortato, Investigation of the inhibition effect of indole-3- carboxylic acid on the copper corrosion in 0.5 M H_2SO_4, Corros. Sci. 50 (2008) 3467–3474.
[28] M. Lebrini, F. Robert, H. Vezin, C. Roos, Electrochemical and quantum chemical studies of some indole derivatives as corrosion inhibitors for C38 steel in molar hydrochloric acid, Corros. Sci. 52 (2010) 3367–3376.
[29] I.L. Rozendeld, Corrosion Inhibitors, McGraw-Hill, New York, NY, 1981.
[30] S.K. Rangarajan, Adsorption isotherms-microscopic modelling, J. Electroanal. Chem. 82 (1977) 93–132.
[31] X. Wang, H. Yang, F. Wang, An investigation of benzimidazole derivative as corrosion inhibitor for mild steel in different concentration HCl solutions, Corros. Sci. 53 (2011) 113–121.
[32] G. Trabanelli, Corrosion Inhibitors, in: F. Mansfeld (Ed.), Corrosion Mechanism, Mercel Dekker, New York, 1987, pp. 119–163.
[33] S. Sankarapapavinasam, F. Pushpanaden, M.F. Ahmed, Piperidine, piperidones and tetrahydrothiopyrrones as inhibitors for the corrosion of copper in H_2SO_4, Corros. Sci. 32 (1991) 193–203.
[34] F. Bentiss, M. Traisnel, M. Lagrenee, The substituted 1,3,4-oxadiazoles: a new class of corrosion inhibitors of mild steel in acidic media, Corros. Sci. 42 (2000) 127–146.
[35] A.Y. Musa, A.A.H. Kadhum, A.B. Mohamad, M.S. Takriff, A.R. Daud, S.K. Kamarudin, On the inhibition of mild steel corrosion by 4-amino-5-phenyl-4H-1, 2, 4-trizole-3-thiol, Corros. Sci. 52 (2010) 526–533.
[36] H.P. Dhar, B.E. Conway, K.M. Joshi, On the form of adsorption isotherms for substitutional adsorption of molecules of different sizes, Electrochim. Acta 18 (1973) 789–798.
[37] B.G. Ateya, Adsorption of thiosemicarbazide on iron cathodes, J. Electroanal. Chem. 76 (1977) 191–198.
[38] E. Kamis, F. Bellucci, R.M. Latanision, E.S.H. El-Ashry, Acid corrosion inhibition of nickel by 2-(triphenosphoranylidene) succinic anhydride, Corrosion 47 (1991) 677–686.
[39] I.J. Pachter, D.E. Zacharias, O. Ribeiro, Indole Alkaloids of Acer saccharinum (the Silver Maple), Dictyoloma incanescens, Piptadenia colubrina, and Mimosa hostiles, J. Org. Chem. 24 (1959) 1285–1287.
[40] W.H. Ailor, Handbook on Corrosion Testing and Evaluation, John Wiley and Sons, Inc., New York, 1971.
[41] H. Vaidyanathan, H. Hackermann, Effect of furan derivatives on the anodic dissolution of Fe, Corros. Sci. 11 (1971) 737–750.
[42] Lj.M. Vračar, D.M. Dražić, Adsorption and corrosion inhibitive properties of some organic molecules on iron electrode in sulfuric acid, Corros. Sci. 44 (2002) 1669–1680.
[43] X. Li, S. Deng, G. Mu, H. Fu, F. Yang, Inhibition effect of nonionic surfactant on the corrosion of cold rolled steel in hydrochloric acid, Corros. Sci. 50 (2008) 420–430.
[44] T.P. Hoar, R.P. Khera, Proceedings 1st Europ Symp. on Corrosion Inhibitors, Ferrara, Italy, 1960. 73.
[45] S.S. Abdel Rehim, O.A. Hazzazi, M.A. Amin, K.F. Khaled, On the corrosion inhibition of low carbon steel in concentrated sulphuric acid solutions. Part I: chemical and electrochemical (AC and DC) studies, Corros. Sci. 50 (2008) 2258–2271.
[46] O.E. Barcia, O.R. Mattos, Reaction model simulating the role of sulphate and chloride in anodic dissolution of iron, Electrochim. Acta 35 (1990) 1601–1608.
[47] P. Li, J.Y. Lin, K.L. Tan, J.Y. Lee, Electrochemical impedance and X-ray photoelectron spectroscopic studies of the inhibition of mild steel corrosion in acids by cyclohexylamine, Electrochem. Acta 42 (1997) 605–615.
[48] A. López, S.N. Simison, S.R. de Sánchez, The influence of steel microstructure on CO2 corrosion. EIS studies on the inhibition efficiency of benzimidazole, Electrochem. Acta 48 (2003) 845–854.
[49] H. Ashassi-Sorkhabi, N. Ghalebsaz-Jeddi, F. Hashemzade, H. Jahani, Corrosion inhibition of carbon steel in hydrochloric acid by some polyethylene glycols, Electrochim. Acta 51 (2006) 3848–3858.
[50] E. Barsoukov, J.R. Macdonald, Impedance Spectroscopy, J. Wiley Sons, Hoboken, New Jersey, 2005.
[51] P. Zoltowski, On the electrical capacitance of interfaces exhibiting constant phase element behaviour, J. Electroanal. Chem. 443 (1998) 149–154.
[52] C.H. Hsu, F. Mansfeld, Concerning the conversion of the constant phase element parameter Y_0 into a capacitance, Corrosion 57 (2001) 747–748.
[53] A. Benedetti, P. Sumodjo, K. Nobe, P.L. Cabot, W.G. Proud, Electrochemical studies of copper copper-aluminium and copper-aluminium-silver alloys: impedance results in 0.5 M NaCl, Electrochem. Acta 40 (1995) 2657–2668.
[54] F.B. Growcock, R.J. Jasinski, Time-resolved impedance spectroscopy of mild steel in concentrated hydrochloric acid, J. Electrochem. Soc. 136 (1989) 2310–2314.
[55] S.L. Li, Y.G. Wang, S.H. Chen, R. Yu, S.B. Lei, H.Y. Ma, De X. Liu, Some aspects of quantum chemical calculations for the study of Schiff base corrosion inhibitors on copper in NaCl solutions, Corros. Sci. 41 (1999) 1769–1782.
[56] A.M. Abdel-Gaber, B.A. Abd-El-Nabey, I.M. Sidahmed, A.M. El-Zayady, M. Saadawy, Inhibitive action of some plant extracts on the corrosion of steel in acidic media, Corros. Sci. 48 (2006) 2765–2779.
[57] P.N. Clark, E. Jackson, M. Robinson, Effect of thiourea and some of its derivatives on the corrosion behaviour of nickel in 50% v/v (5.6 M) hydrochloric acid, Br. Corros. J. 14 (1979) 33–39.
[58] M. Abdallah, Rhodanine azosulpha drugs as corrosion inhibitors for corrosion of 304 stainless steel in hydrochloric acid solution, Corros. Sci. 44 (2002) 717–728.
[59] J. de Damborenea, J.M. Bastidas, A.J. Vázquez, Adsorption and inhibitive properties of four primary aliphatic amines on mild steel in 2 M hydrochloric acid, Electrochim. Acta 42 (1997) 455–459.
[60] O.L. Riggs Jr., R.M. Hurd, Temperature coefficient of corrosion inhibition, Corrosion 23 (1967) 252–258.
[61] A.K. Singh, M.A. Quraishi, Inhibiting effects of 5-subtituted isatin-based Mannich bases on the corrosion of mild steel in hydrochloric acid solution, J. Appl. Electrochem. 40 (2010) 1293–1306.
[62] F. Donahue, K. Nobe, Theory of organic corrosion inhibitors, J. Electrochem. Soc. 112 (1965) 886–891.
[63] M. Lagrenee, B. Mernari, M. Bouanis, M. Traisnel, F. Bentiss, Study of the mechanism and inhibiting efficiency of 3,5-bis(4-methylthiophenyl)-4H-1,2,4-triazole on mild steel corrosion in acidic media, Corros. Sci. 44 (2002) 573–588.
[64] J.O'.M. Bockris, A.K.N Reddy, Modern Electrochemistry, Third Printing Vol. 2, Plenum Press, New York, 1972.
[65] G. Schmitt, in: Proceedings 6th Europ. Symp. on Corrosion Inhibitors, Ferrara, Italy, 1985 (appendix).